Fluorescence Study of Conformational Flexibility of RNase S-Peptide: Distance-Distribution, End-to-End Diffusion, and Anisotropy Decays†

B. P. Maliwal and J. R. Lakowicz*

Center for Fluorescence Spectroscopy, Department of Biological Chemistry, University of Maryland School of Medicine, 108 North Greene Street, Baltimore, Maryland 21201

G. Kupryszewski and P. Rekowski

Institute of Chemistry, University of Gdańsk, Gdańsk, Poland

Received June 23, 1993; Revised Manuscript Received August 23, 1993®

ABSTRACT: Frequency-domain fluorescence resonance energy transfer and anisotropy measurements were performed to characterize conformational dynamics of an analog of the RNase S-peptide (residues 1–20). Trp was used as a donor by replacing Phe 8, and a dansyl acceptor group was introduced at position 1 or 18. The distance-distribution parameters, half width of the distribution, end-to-end diffusion coefficient, and to some extent anisotropy decays were sensitive to changes in the S-peptide conformation. The observed mean distance of about 13–14 Å between residues 1 and 8 in the presence of 50% TFE and when bound to RNase S-protein is in reasonable accord with the X-ray structure of RNase. The mean distance of 9.3 Å between residues 8 and 18 in the presence of 50% TFE is, however, significantly smaller than 15.3 Å found for the S-protein complex. The half-width of the distance distribution increased from about 9 to 18 Å for residues 1–8 and from about 6 to 14 Å for segment 8–18 with the loss of helical structure. The half-widths of 9 Å in the case of 1–8 segment when peptide is helical suggests the presence of considerable conformational heterogeneity. Also, the 14 Å half-width for segment 8–18 when it is random-coil is smaller than that expected for a random coil 11-residue segment. The donor-to-acceptor diffusion coefficients were less than 1×10^{-7} cm^2/s at 2 °C for both segments and increased to $1–2 \times 10^{-6}$ cm^2/s at 35 °C. The anisotropy decays reveal the S-peptide to be rather rigid at 2 °C irrespective of the conformation and the peptide becomes flexible upon raising the temperature to 35 °C. The results also indicate small but significant differences between two segments in their conformational dynamics. Overall, the results suggest that the specific amino acid sequence will significantly influence the relationship between distance distribution parameters and conformational dynamics in case of short peptides. Also, these results suggest that distance-distribution measurements and anisotropy decays are a valuable tool to characterize conformational dynamics of short peptides.

Since the early seminal work of Anfinsen and co-workers, it has been recognized that the amino acid sequence of a polypeptide chain contains much of the information required for correct folding (Anfinsen, 1973). The experimentally observed folding of proteins is a rapid and cooperative process which suggests that it cannot occur by a random search of all possible conformations. For a protein made up of 100 amino acids, it would take on the order of 10^{50} years or longer to search all possible conformations (Levinthal, 1968). It is now generally accepted that protein folding occurs via local folded intermediate sites (Wetlaufer, 1981; Kim & Baldwin, 1982; Gierasch & King, 1989; Barrick & Baldwin, 1993). However, it has been difficult to identify these transient structures during folding as the process is very rapid and cooperative. In principle, it should be possible to identify the peptide sequences which form the initiation sites and to characterize the secondary structure in the isolated short peptides. However, early efforts to observe secondary structure in isolated linear peptide fragments proved quite unsuccessful. At least part of this failure was due to rather insensitive techniques available as these secondary structures are transient and make up only a small fraction of the total peptide population. Furthermore, the helix–coil transition theory (Zimm & Bragg, 1959; Quian & Schellman, 1992) based on the parameters from host–guest studies (Sueiki et al., 1984) also suggested that the small peptides (smaller than 20 residues) are unable to form secondary structure. Among the exceptions were the C-peptide (residues 1–13) and S-peptide (residues 1–20) from RNase which showed the temperature and pH-dependent presence of an α-helix (Brown & Klee, 1971). More recently, working primarily with two dimensional (2D) NMR, the transient presence of secondary structure elements has been observed in several linear peptide fragments (Wright et al., 1988; Montelione & Scheraga, 1989; Jaenicke, 1991) as well as in de novo synthetic peptides (Scholtz et al., 1991; Merutka et al., 1991; Gans et al., 1991).

Since the observation of Brown and Klee (1971), extensive studies on helix formation in both C-peptide and S-peptide and their analogs have been carried out using circular dichroism (CD) and NMR. The helix was found to be stabilized by specific side-chain interactions including salt-bridge formation between Glu 2^- and Arg 10^+ (Bierzynski et al., 1982; Shoemaker et al., 1985; Rico et al., 1986), aromatic interactions between Phe 8 and His 12^+ (Rico et al., 1986; Shoemaker et al., 1990), and interactions of N-terminal charged groups with the helix dipole (Shoemaker et al., 1987). The helix is extended from residue 3 to 13 (Filippi et al., 1978; Rico et al., 1986; Nelson & Kallenbach, 1989). Effects of

† This work was supported by Grants GM-35154 and TW-00049 (J.R.L.) from the National Institutes of Health, with support for instrumentation from the National Science Foundation, DIR 8710401 (J.R.L.) and the NIH RR 08119 (J.R.L.).

* Correspondence should be addressed to this author.

® Abstract published in *Advance ACS Abstracts,* October 15, 1993.

0006-2960/93/0432-12337$04.00/0

amino acid substitutions on the conformation of C-peptide and S-peptide and their complexes with the S-protein have also been reported (Filippi et al., 1976, 1978; Rico et al., 1986; Strehlow & Baldwin, 1989; Connelly et al., 1990). 2D NMR measurements on C-peptide analogs suggested a conformational ensemble consisting of three major populations of extended, helical and the third with a salt bridge between Glu 2^- and Arg 10^+ (Osterhout et al., 1989).

Fluorescence resonance energy transfer (FRET)[1] can also provide significant insight into the conformational dynamics of biological macromolecules. In their pioneering work, Steinberg and co-workers showed how time-resolved FRET can be effectively used to recover distance distributions and end-to-end diffusion coefficients by monitoring donor fluorescence intensity decays (Grinvald et al., 1972; Haas et al., 1975, 1978). These methods have been further extended in this laboratory (Lakowicz et al., 1988, 1990, 1992; Cheung et al., 1991a,b; Eis & Lakowicz, 1993) and by Scheraga, Haas and co-workers (Amir and Haas, 1988; Haas et al., 1988; Beals et al., 1991) to study conformational dynamics of several polypeptides and proteins. In time-resolved FRET the conformational distribution is recovered as the mean distance ($\bar{r}$) with a half-width of the distribution of donor-to-acceptor distances (hw) and a donor-to-acceptor diffusion coefficient (D). The hw of the distribution is related with the conformational heterogeneity as the distribution profile becomes wider with increasing disorder. Similarly, as D has contributions from both the internal restraint of the linker chain and the viscous drag of the solvent, it can also increase with an increase in conformational disorder. For example, in case of melittin the half-width increased from 8 Å to 30 Å for segments 1–19 upon going from the α-helical to random coil state (Lakowicz et al., 1990). Similarly, the value of D in the case of segments 133–158 of troponin I increased by about 10-fold upon denaturation (Lakowicz et al., 1992). Some complementary information on the flexibility can also be obtained from fluorescence anisotropy measurements of suitably located fluorophores (Steiner, 1991). For example, the anisotropy decays of Trp 19 in the case of melittin are dominated by overall peptide motions in helical state while the local motions are dominant in random coil form (Lakowicz et al., 1990).

In present paper we describe the conformational dynamics of S-peptide under a variety of experimental conditions using frequency-domain FRET and fluorescence anisotropy measurements. In this analog of S-peptide the Phe 8 was replaced by Trp to serve as the fluorescence donor. A dansyl group which served as the acceptor was introduced at α-amino group of Lys 1 or at position 18 as dansyl diaminopropionic acid [Dap(dns)] in place of Ser 18. By selecting appropriate experimental conditions, we were able to observe S-peptide as it gradually changed from a highly helical form to an extended random coil.

MATERIALS AND METHODS

Peptide Synthesis and Purification. N^{α}-*tert*-Butyloxycarbonyl-N^{β}-dansyl-L-α,β-diaminopropionic acid and N^{ϵ}-dansyl-N^{α}-benzyloxycarbonyl-L-lysine were prepared by the standard methods. All the remaining amino acid derivatives were obtained from Fluka AG. The peptides [Trp^8]peptide S, [Lys-(dns)^1,Trp^8]peptide S, and [Trp^8,Dap(dns)^{18}]peptide S were synthesized by the solid-phase method using Boc protection chemistry. The peptide were cleaved from the resin by "low–high" HF procedure. The crude peptides were desalted on Sephadex G-25 Column in 25% acetic acid. The pertinent fractions were lyophilized and chromatographed on preparative HPLC on a reverse-phase Vydac C_{18} column (15–20 μm particle size), with an acetonitrile gradient in 0.1% trifluoroacetic acid (10–15%) to yield pure S-peptide analogs. The purified peptides were analyzed for amino acid composition which gave the expected results. The S-peptides were further purified before the experiments by analytical HPLC on a reverse-phase C_{18} Beckman Ultrasphere column (5-μm particle size) using 0.1% trifluoroacetic acid and acetonitrile. A mixture of the three purified peptides was run on a 5–35% acetonitrile gradient on an analytical HPLC column. This analysis showed complete separation of the peptides and the purity of each peptide (not shown).

Fluorescence Measurements. The buffer system used in all the experiments consisted of 50 mM appropriate buffer (citrate, MOPS, or Tris) containing 50 mM NaCl. The steady-state spectra and the quantum yield measurements were carried out by exciting a 0.1 OD solution at 287 nm using a SLM 8000 photon counting instrument with slit widths of 4 and 8 nm, respectively, for excitation and emission. An aqueous solution of tryptophan (quantum yield = 0.13) was used as a reference. The frequency-domain measurements were carried out on a previously described 10-GHz instrument (Laczko et al., 1990). The excitation source was a 3.79 MHz train of 5-ps wide pulses obtained from the cavity dumped output of a synchronously pumped rhodamine 6G dye laser. The dye laser output was frequency doubled to either 287 nm for lifetime or 297 nm for anisotropy measurements. This intrinsically modulated source was used to excite the sample and the fluorescence emission collected through a Schott 340-nm interference filter was detected by a microchannel plate photomultiplier tube. The temperatures were controlled to an accuracy of ±1 °C. The measurements were also carried out in the presence of an external quencher acrylamide (0.2–0.3 M) and the data analyzed globally to improve resolution in both distance-distribution measurements (Lakowicz et al., 1991) and anisotropy decays (Gryczynski et al., 1988). The donor-only peptide concentrations were typically 40–50 μM while those of donor–acceptor peptides were near 100 μM. At these peptide concentrations, the background fluorescence was less than 1%.

Somewhat different conditions were used to study the complex of S-peptide with S-protein (Sigma Chemical Co.). The S-peptide and S-protein concentrations were 50 and 100 μM, respectively. The excitation wavelength was 292 nm and the emission observed through a Corning 7-60 filter. The intensity decay measurements to recover distance distribution were carried out in presence of 0.22 M acrylamide. These experimental conditions were selected to minimize the contribution of tyrosine fluorescence from S-protein. The use of 0.22 M acrylamide allowed us to selectively quench the tyrosine fluorescence, and the 292 nm excitation selected mostly the tryptophan residue. It should be noted that most of the tyrosine fluorescence in RNase is from the surface residues, and these residues are highly accessible to acrylamide. On the other hand, Trp 8 being buried in the complex as seen by a 20-nm blue-shift in the emission becomes significantly inaccessible to acrylamide (results not shown).

[1] Abbreviations: CD, circular dichroism; dns, dansyl; Dap, diaminopropionic acid; FRET, fluorescence resonance energy transfer; Lys-(dns), dansyl lysine; OD, optical density; RNase, ribonuclease; TFE, trifluoroethanol.

THEORY

The donor intensity decays in the absence of the acceptor were fit to a sum of exponentials

$$I_D(t) = I_{0D}\sum_i \alpha_{Di} \exp(-t/\tau_{Di}) \quad (1)$$

where I_{0D} is the intensity of the donor emission at time t = 0 and α_{Di} are the fractional intensities of the components characterized by the decay times τ_{Di}. The fractional intensity (f_i) of each lifetime component in the decay is given by $\alpha_i\tau_i/\sum_j\alpha_j\tau_j$ and the average lifetime $\langle\tau\rangle$ by $\sum_i f_i\tau_i$. The values of α_{Di} are normalized so that $\sum_i\alpha_{Di} = 1.0$. We assume that the Förster distance (R_0) for energy transfer from each component in the donor decay is the same as in the case of a single-exponential donor with the same lifetime (Lakowicz et al., 1988). Due to the distance distributions, the donor decay in presence of an acceptor will be nonexponential and will contain contributions from all the allowed conformers with different donor to acceptor distances. The donor decays under such conditions can be described by

$$I_{DA}(t) = I_{DAO}\sum_i \alpha_{Di}\int_{r_{min}}^{r_{max}} N_0(r)\overline{N^*}_i(r,t)\,dr \quad (2)$$

where r_{min} and r_{max}, respectively are the distance of the closest approach and the distance between probes for fully extended structure, and $N_0(r)$ denotes the donor–acceptor distance distribution of the excited molecules at $t = 0$. In practice, the values of r_{min} and r_{max} are chosen sufficiently small and large, respectively, so that the distance-distribution analysis is not sensitive to the precise values. The time- and distance-dependent population of excited donors in the case of a flexible donor–acceptor pair can be described by the function $N^*_i(r,t)$ as follows (Haas et al., 1978).

$$\frac{\partial \bar{N}^*_i(r,t)}{\partial t} = -\left[\frac{1}{\tau_{Di}} + \frac{1}{\tau_{Di}}\left(\frac{R_0}{r}\right)^6\right]\bar{N}^*_i(r,t) + \frac{1}{N_0(r)}\frac{\partial}{\partial r}\left[N_0(r)D\frac{\partial \bar{N}^*_i(r,t)}{\partial r}\right] \quad (3)$$

Here D is the acceptor-to-donor diffusion coefficient. We assumed a Gaussian model for the initial distance distribution of the excited molecules where

$$N_0(r) = \begin{cases} \frac{N}{Z}\exp[-(r-R_{av})^2/(2\sigma^2)] & \text{for } r_{min} \le r \le r_{max} \\ 0 & \text{elsewhere} \end{cases} \quad (4)$$

R_{av} and $\sigma = hw/\sqrt{8}(\ln 2)$ are the average distance and standard deviation of the untruncated Gaussian function, respectively. In the case of distance distribution without intramolecular diffusion, D is set to zero which results in cancellation of the last term on the right-hand side of eq 2. A detailed account of the distance-distribution and data analysis is given elsewhere (Haas et al., 1978; Lakowicz et al., 1988, 1991, 1993; Kuśba & Lakowicz, 1993).

In the case of a flexible molecule the anisotropy decays [$r(t)$] can be described as a sum of exponentials

$$r(t) = \sum_i r_i \exp(-t/\theta_i) \quad (5)$$

where θ_i are the rotational correlation times and r_i are the associated anisotropies. A detailed account of theory and data analysis of frequency domain intensity and anisotropy decays are given elsewhere (Lakowicz et al., 1984; Maliwal & Lakowicz, 1986). The experimental error in phase angles and modulation were estimated from the random error in the data. In the case of the intensity decays, the errors were about 0.2–0.3° in phase and about 0.004–0.005 in modulation. The errors were somewhat larger at the highest frequencies. Similarly, the value of errors were about 0.2° in differential phase angles and 0.01 in modulated anisotropies in the case of anisotropy decay measurements.

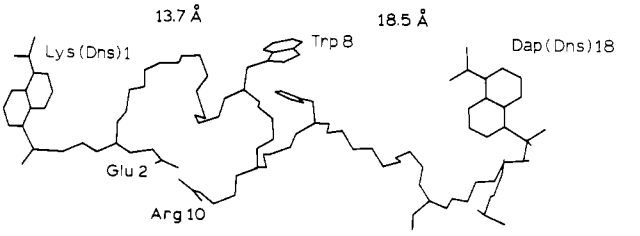

FIGURE 1: View of S-peptide analog based on crystal structure of RNase. Note that Trp 8 and DAP(dns)18, respectively, replaced Phe 8 and Ser 18 and a dansyl group is present at the α-amino end of Lys 1. The distances are between α-carbons of residues 1 and 8 and 8 and 18, respectively. The experimental peptides contained only one dns acceptor.

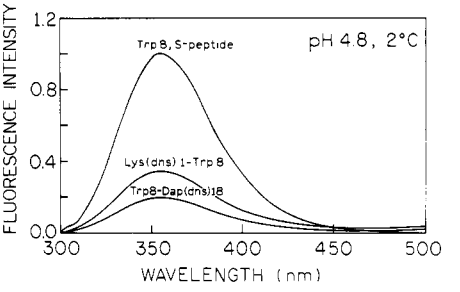

FIGURE 2: Steady-state emission spectra of donor and donor-acceptor S-peptides at pH 4.8, 2 °C. The excitation wavelength was 287 nm.

RESULTS

A representation of S-peptide analogue is shown in Figure 1. This is based on the crystal structure of RNase with replacement of Phe 8 by Trp 8, Ser 18 by Dap(dns)18, and introduction of dansyl moiety at α-amino group of Lys 1. Evident in the figure are the helical region extending from residues 3 to 13, the aromatic interaction between His 12 and Trp 8 (analogous to His and Phe), and the salt bridge between Glu 2 and Arg 10. Representative steady-state spectra (pH 4.8, 2 °C) of S-peptide with and without the presence of acceptors are shown in Figure 2. The uncorrected maxima for tryptophan emission is about 356–357 nm, which suggests an exposed tryptophan residue. There is considerable energy transfer in the presence of dansyl group as seen by the significant decrease in the emission intensity. Similar trends in the energy transfer mediated decrease in the tryptophan intensities were also observed under all experimental conditions (results not shown). The emission maxima and the general shape of emission spectra for S-peptide were similar in the absence and presence of the acceptor group. This would suggest that introduction of dansyl moiety is not causing any change in the environment of the donor tryptophan residue. The emission maxima were similar at pH 4.8 and 8.0 and at pH 7.0 in the presence of 6 M GuHCl. There was an 8–10-nm blue-shift in the presence of 50% trifluoroethanol (TFE) and about 20-nm blue-shift when the S-peptide formed a complex with S-protein.

The intensity of donor-only S-peptide was also sensitive to the experimental conditions. We observed a biphasic increase in the emission intensity between pH 3.0 and 8.0 (results not shown). The increase between pH 3.0 and 5.0 most likely

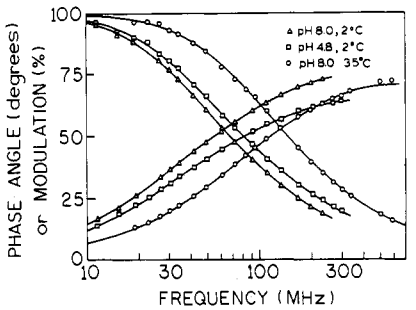

FIGURE 3: Representative frequency domain tryptophan intensity decays of donor only S-peptides. The experimental conditions are pH 8.0, 2 °C (△), pH 4.8, 2 °C (□), and pH 8.0 at 35 °C (○).

Table I: Multicomponent Analysis of Tryptophan Intensity Decays of Donor Only S-Peptide[a]

experimental conditions	T (°C)	two[b] τ_i (ns)	two[b] f_i	three τ_i (ns)	three f_i	$\langle\tau\rangle$ (ns)	χ_R^2 2τ	χ_R^2 3τ
pH 8.0, 50% TFE	2	3.68	0.84	4.13	0.69	3.28	4.36	1.28
		0.83	0.16	1.53	0.28			
				0.03	0.03			
pH 4.8	2	3.95	0.85	4.40	0.72	3.50	5.61	1.04
		0.61	0.15	1.39	0.23			
				0.13	0.05			
pH 8.0	2	4.61	0.86	4.90	0.77	4.17	1.95	0.63
		0.17	0.14	1.86	0.21			
				0.09	0.02			
pH 8.0	35	2.02	0.92	2.64	0.45	1.94	3.35	1.19
		0.34	0.08	1.46	0.51			
				0.13	0.04			
pH 7.0, 6 M GuHCl	2	4.46	0.85	4.83	0.72	3.98	3.04	1.05
		1.13	0.15	1.92	0.26			
				0.03	0.02			
pH 7.0, 6 M GuHCl	35	2.48	0.84	2.59	0.77	2.21	1.51	0.68
		0.70	0.16	0.98	0.22			
				0.04	0.01			

[a] The S-peptides were excited at 287 nm and the emission measured through a Schott WG305 and 340-nm interference filters. [b] Number of components in the multiexponential analysis.

reflects ionization of Glu 9 while that between pH 5.0 and 8.0 is due to deprotonation of His 12. The intensity was moderately lower in the presence of 50% TFE, and it was significantly quenched in the complex with S-protein. As expected, the emission intensity decreased when the temperature was raised to 35 °C.

Multicomponent Analysis of Intensity Decays

Some examples of frequency-dependent phase and modulation for donor only S-peptide tryptophan intensity decays are shown in Figure 3. These decays were measured at 2 °C at pH 8.0 and 4.8 and at 35 °C at pH 8.0. All the frequency-dependent phase and modulation profiles in Figure 3 indicate that the intensity decays are heterogeneous. Similar heterogeneity in the donor decays was observed under all the experimental conditions (results not shown), and the decays could be satisfactorily described by three lifetime components. These results are summarized in Table I. At 2 °C, the first lifetime was in the range of 4–5 ns, the second about 2 ns, and the third less than 0.15 ns. Also given in Table I are average lifetimes which follow the general trend seen in the steady-state intensities. For example, at 2 °C average lifetime increased from 3.5 ns at pH 4.8 to 4.2 ns at pH 8.0, and decreased from 4.2 to 2.0 ns at pH 8.0 upon raising the temperature to 35 °C.

The distribution of distances in energy transfer results in a range of transfer rates for the donor depending on the acceptor position. This leads to nonexponential donor decays and forms the basis of the recovery of the distance-distribution parameters (Grinvald et al., 1972; Haas et al., 1975). The donor intensity decays therefore should be more heterogeneous in the presence of energy transfer if there is a distribution of distances between the donor and acceptor moieties. To this end, a multicomponent lifetime analysis of the intensity decays of the donor and donor–acceptor pairs was carried out, and the relative improvement in the χ_R^2 values for two- and three-component fits were examined. Some examples are given in Table II. These analyses indeed demonstrate that intensity decays in the presence of energy transfer are more heterogeneous. For example, at pH 8.0 in presence of 50% TFE, the ratio of χ_R^2 for two- and three-component analyses increases from 3.4 for donor alone to 14.2 and 12.4 for the donor and acceptor-labeled peptides due to energy transfer. A similar trend was observed for other experimental conditions (results not shown).

Table II: Representative Multicomponent Analysis of Tryptophan Intensity Decays of S-Peptide Labeled with Dansyl Group

sample	two τ_i (ns)	two f_i	three τ_i (ns)	three f_i	$\langle\tau\rangle$ (ns)	χ_R^2 2τ	χ_R^2 3τ	$\chi_{2\tau}^2/\chi_{3\tau}^2$
(A) pH 8, 50% TFE, 2 °C								
Trp 8	3.68	0.84	4.13	0.69	3.28	4.36	1.28	3.4
	0.83	0.16	1.53	0.28				
			0.03	0.03				
Lys(dns)1–Trp 8	1.71	0.76	2.22	0.51	1.44	12.80	0.90	14.2
	0.29	0.24	0.73	0.41				
			0.08	0.08				
Trp 8–Dap(dns)18	1.41	0.66	2.81	0.30	1.21	37.22	3.0	12.4
	0.19	0.34	0.64	0.55				
			0.08	0.15				
(B) pH 7.0, 6 M GuHCl, 35 °C								
Trp 8	2.48	0.84	2.59	0.77	2.21	1.51	0.68	2.2
	0.70	0.16	0.98	0.22				
			0.03	0.01				
Lys(dns)1–Trp 8	1.64	0.82	1.83	0.66	1.43	2.58	0.61	4.2
	0.42	0.18	0.76	0.30				
			0.13	0.04				
Trp 8–Dap(dns)18	1.24	0.77	1.51	0.48	1.05	2.38	0.49	4.9
	0.34	0.23	0.70	0.45				
			0.15	0.07				

Table III: Distance-Distribution Parameters and the End-to-End Diffusion Coefficients for Lys(dns)1–Trp 8 Segment of the S-Peptide

experimental condition	T (°C)	R_0 (Å)	$\bar{r}$ (Å)[a]	hw (Å)[b]	D (10^{-7} cm^2/s)[c]	χ_R^2
S-protein complex	1	16.5	14.9 ± 0.4	8.6 ± 1.3	<1.0	0.88
50% TFE, pH 8	2	17.5	13.3 ± 0.4	11.0 ± 1.0	1.7 ± 0.7	1.19
pH 4.8	2	17.8	13.5 ± 0.4	14.4 ± 0.8	<1.0	1.17
pH 8.0	2	18.5	12.8 ± 0.8	17.8 ± 1.2	4.4 ± 1.0	0.48
pH 8.0	35	15.9	13.2 ± 0.7	18.1 ± 2.8	12.6 ± 3.7	0.73
6 M GuHCl, pH 7.0	2	18.0	19.1 ± 0.1	8.7 ± 0.6	<1.0	0.88
6 M GuHCl, pH 7.0	35	15.7	18.6 ± 0.3	18.5 ± 2.7	21.0 ± 5	0.69

[a] Mean of the distance-distribution. [b] Half-width of the distance-distribution. [c] Donor-to-acceptor diffusion coefficient. 1×10^{-7} cm^2/s is equivalent to 1 Å^2/ns.

Distance-Distribution Analysis

The calculated values of the Förster distances and experimentally recovered mean distance ($\bar{r}$), the half-width of distribution (hw) and the end-to-end diffusion coefficient (D) are given in Table III for Lys(dns)1-Trp8 segment and in Table IV for Trp 8-Dap(dns)18 segment. The values of the Förster distance calculated from the spectral parameters were about 18 Å at 2 °C and about 16 Å at 35 °C. In calculating

Table IV: Distance-Distribution Parameters and the End-to-End Diffusion Coefficients of the Trp 8–Dap(dns)18 Segment of the S-Peptide

experimental conditions	T (°C)	R_0 (Å)	$\bar{r}^a$ (Å)	hw^b (Å)	D^c (10^{-7} cm^2/s)	χ_R^2
S-protein complex	1	16.5	15.3 ± 0.2	6.0 ± 1.0	<1.0	0.83
50% TFE, pH 8.0	2	17.5	9.3 ± 0.4	10.6 ± 0.5	<1.0	2.70
pH 4.8	2	17.8	10.8 ± 0.4	12.4 ± 0.6	<1.0	1.65
pH 8.0	2	18.5	13.9 ± 0.4	12.2 ± 1.1	3.8 ± 1.0	0.82
pH 8.0	35	15.9	12.4 ± 0.5	12.8 ± 1.4	8.6 ± 2.6	1.00
6 M GuHCl, pH 7.0	2	18.0	16.4 ± 0.1	5.3 ± 0.3	<1.0	0.79
6 M GuHCl, pH 7.0	35	15.7	14.9 ± 0.1	13.8 ± 1.2	16.4 ± 2.6	0.65

[a] Mean of the distance-distribution. [b] Half-width of the distance-distribution. [c] Donor-to-acceptor diffusion coefficient.

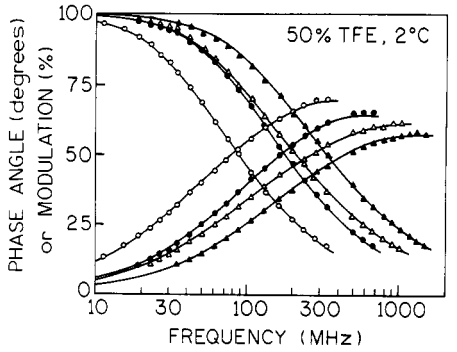

FIGURE 4: Distance-distribution fits to frequency dependent phase and modulation in the case of Lys(dns)1–Trp 8 segment, 50–60% helical conformation, 50% TFE at 2 °C. The donor-only intensity decays are given by open symbols (○, △). The figure also includes decays obtained in the presence of external quencher acrylamide (●, ▲).

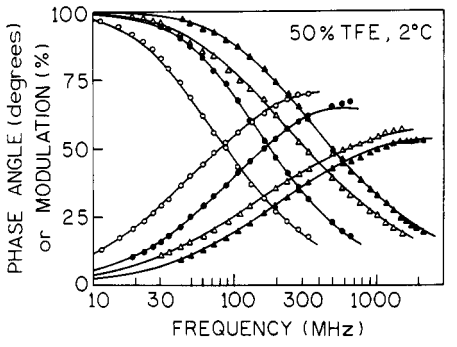

FIGURE 5: Distance-distribution fits to frequency responses for Trp 8–Dap(dns)18 segment. The conditions and symbols are the same as those in Figure 4.

R_0 values, we used a κ^2 of $^2/_3$ for several reasons. As shown in the anisotropy measurements, the tryptophan has considerable motional freedom. The acceptor dansyl groups should have even more motional freedom as they are located at or near the terminal ends of the peptide [see results for melittin, Lakowicz et al. (1990)]. This motional freedom of the donor and the acceptors and the mixed character of the electronic transitions in the case of acceptor dansyl group should result in a κ^2 close to that of dynamic limit. Furthermore, any error in R_0 will only affect $\bar{r}$ and not alter the distribution half-widths. The uncertainties (at 67% confidence limit), given in the Tables III and IV, were calculated, taking into account correlations among the parameters (Johnson, 1983). Some representative distance-distribution analyses for frequency domain intensity decays are given in Figure 4 (segment 1–8) and Figure 5 (segment 8–18). These frequency responses were observed in the presence of 50% TFE at 2 °C and 6 M GuHCl at 35 °C for both of the segments. The fits are satisfactory and suggest that the distance-distribution model used can adequately describe donor intensity decays in the presence of energy transfer. A few observations can be made about Figures 4 and 5. In both cases, in the presence of 50% TFE and for other experimental conditions (not shown), the donor intensity decays in the absence of acceptor are heterogeneous, and the heterogeneity increases in the presence of acceptor. The energy transfer results in shortening of the donor lifetime, which is reflected as a shift to higher frequencies. The extent of energy transfer is less in the case of 1–8 segment compared to 8–18 segment and is indicated by the relative magnitude of the frequency shifts. The energy transfer in both segments appear to be more similar at 35 °C in the presence of 6 M GuHCl (not shown).

Lys(dns)1–Trp8 Segment. First we describe the results from the distance-distribution analysis for Lys(dns)1–Trp 8 segment (Table III). Recall that under the experimental conditions employed, the S-peptide conformation ranges from 50–60% helical (50% TFE, 2 °C, and S-protein complex, 1 °C) to the disordered state (6 M GuHCl at 2 and 35 °C and pH 8.0 at 35 °C) (Filippi et al., 1978; Rico et al., 1986; Nelson & Kallenbach, 1986; Shoemaker et al., 1987). The recovered values of diffusion coefficients were smaller than 1×10^{-7} cm^2/s at 2 °C in the cases of pH 4.8, 6 M GuHCl, and S-protein complex. The value of diffusion coefficients varied between 1.6×10^{-7} cm^2/s in the presence of 50% TFE at 2 °C and 2.1×10^{-6} cm^2/s in the presence of 6 M GuHCl at 35 °C. There seems to be some trend of increased diffusion coefficients with a decrease in the secondary structure. For example, going from pH 4.8 to 8.0 at 2 °C and from 2 to 35 °C at pH 8.0 resulted in a several-fold increase in the value of D. The hw value also showed a modest increase with the loss of secondary structure. The hw increased from 8.6 Å in S-protein complex and 11 Å in the presence of 50% TFE to about 18 Å at 35 °C (pH 8.0 and 6 M GuHCl) when S-peptide changed from 50–60% helical structure to random coil. A surprising behavior was seen at 2 °C in the presence of 6 M GuHCl where the observed distribution was comparable to that in the case of S-protein complex. It is surprising because the S-peptide is a random coil in the presence of 6 M GuHCl and is expected to show a wider distribution. The average distance between the donor and acceptor in the segment 1–8 did not significantly change with secondary structure except in the presence of 6 M GuHCl when it increased by 4–5 Å. The values of the mean distance were between 13 and 15 Å in the S-protein complex, in the presence of 50% TFE, and at pH 4.8 and 8.0.

Trp8–Dap(dns)18 Segment. The results for donor-to-acceptor distance-distribution analysis in the case of residues 8–18 are given in Table IV. The trend in the diffusion coefficient with changes in the secondary structure for the segment 8–18 of S-peptide was also similar to that observed for the 1–8 segment. The diffusion coefficients were smaller than 1×10^{-7} cm^2/s at 2 °C in the presence of 50% TFE, S-protein, 6 M GuHCl, and at pH 4.8. It increased to about 3.8×10^{-7} cm^2/s upon raising the pH to 8.0 at 2 °C. Upon further raising the temperature to 35 °C, a condition which results in complete loss of secondary structure, the value of D increased to about $(1–1.6) \times 10^{-6}$ cm^2/s. In the case of the hw, we observed a narrow distribution for S-protein complex (6 Å) which increased to about 10 Å in the presence of 50% TFE. The hw further increased to about 12 Å at pH 4.8 and 8.0 at 2 °C and to 14 Å in the presence of 6 M GuHCl at 35 °C. Similar to that in the case of segment 1–8, the distribution was quite narrow in the presence of 6 M GuHCl at 2 °C as

Table V: Distance-Distribution Parameters for Segments 1–8 and 8–18 of the S-Peptide from a Global hw Analysis

experimental conditions	T (°C)	residues 1–8				residues 8–18			
		$\bar{r}$ (Å)	hw (Å)	D (10^{-7} cm^2/s)	χ_R^2	$\bar{r}$ (Å)	hw (Å)	D (10^{-7} cm^2/s)	χ_R^2
S-protein complex	1	12.5	15.2	4.6	1.00	14.1	12.4	7.3	1.78
50% TFE, pH 8	2	12.0		4.7	(1.32)[a]	7.7		<1.0	(1.68)[a]
pH 4.8	2	12.9		<1.0	(36.93)[b]	11.1		<1.0	(37.50)[b]
pH 8.0	2	13.8		2.6		13.8		4.1	
pH 8.0	35	13.8		8.8		12.6		8.1	
6 M GuHCl, pH 7.0	2	19.7		4.7		16.2		6.0	
6 M GuHCl, pH 7.0	35	19.1		15.8		15.0		14.8	

[a] Ratio of the sum of separate analysis χ_R^2 vs global hw and variable $\bar{r}$ and D analysis χ_R^2. [b] χ_R^2 value form a global $\bar{r}$, hw, and variable D analysis.

seen in a hw value of 5.3 Å. The value of $\bar{r}$ increased from 9 to 11 Å for more structured forms (50% TFE, pH 4.8, 2 °C) to about 14 Å at pH 8.0 at 2 °C, and further increased to 16.4 Å in the presence of 6 M GuHCl at 2 °C. A decrease in mean distances of about 1–1.5 Å was observed when the temperature was raised from 2 to 35 °C. Surprisingly, the $\bar{r}$ value is significantly different for the S-protein complex (15.3 Å) when compared to that observed in the presence of 50% TFE (9.3 Å), even though their helical contents are similar.

Overall, we observed some changes in the distance-distribution parameters with the changing secondary structure of S-peptide. Generally, loss of secondary structure resulted in somewhat larger hw and D. The order of the increase in the distribution half-width in the case of segment 1–8 was 6 M GuHCl, 2 °C ~ S-protein complex < 50% TFE, 2 °C < pH 4.8, 2 °C < pH 8.0, 2 °C ~ 35 °C ~ 6 M GuHCl, 35 °C. In the case of residues 8–18, the increase in the hw with the experimental condition was in the order 6 M GuHCl, 2 °C ~ S-protein complex < 50% TFE, 2 °C < pH 4.8, 2 °C, ~ pH 8.0, 2 °C ~ 35 °C < 6 M GuHCl, 35 °C. However, we must emphasize that the changes seen are rather modest, and that there are considerable uncertainties in the recovered parameters. In order to evaluate the significance of the observed differences in the recovered parameters, we analyzed all the results for a given segment under different experimental conditions by linking globally in various combinations $\bar{r}$, hw, and D. The χ_R^2 values were larger than 100 when the experimental data sets were fit to a single value of $\bar{r}$, hw, and D for either segment. The very large χ_R^2 value clearly demonstrates that distributions are indeed significantly different under various experimental conditions. It was also not possible to fit the whole set of data for either segment with a global $\bar{r}$ and hw and a variable D which gave χ_R^2 of about 37. However, it was possible to obtain a somewhat satisfactory global hw fit with variable $\bar{r}$ and D for both segments. This trend in χ_R^2 values suggests that the changes observed in the mean distances and the distributions in response to the solution conditions are real and not due to the uncertainties in the intramolecular diffusion. The results from global hw, variable $\bar{r}$, and variable D analysis are given in Table V for both segments. For such analysis the increases in the χ_R^2 values were less than 2-fold when compared to those observed for fits to each data set with variable r, hw, and D. It should be noted that most of the increase in the χ_R^2 value in the global hw fit is seen in the structured forms of S-peptide, and therefore we are actually underestimating the differences. In this global hw fit we still observed a modest increase in D at higher temperature as well as with the loss of secondary structure. Also the magnitude and the trend of changes in $\bar{r}$ with the loss of secondary structure is similar to that observed where r, hw, and D were recovered from analyzing each data set separately. Overall, the results shown in Tables III, IV, and V suggest that the changes occurring in the secondary structure of the S-peptide are reflected in the recovered distance-distribution parameters. However, these results also point to both the significant correlation between hw and D and somewhat modest nature of the changes.

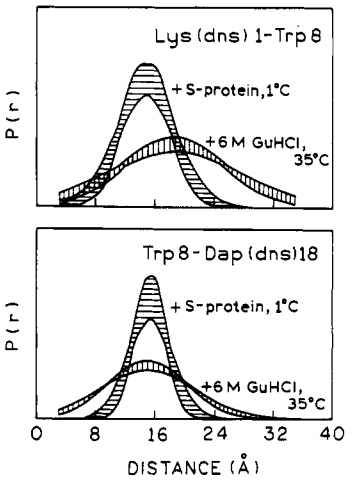

FIGURE 6: Distance-distribution profiles of (top) Lys(dns)1–Trp 8 and (bottom) Trp 8–Dap(dns)18 segments when the peptide is helical (S-protein complex, 1 °C) or random coil (6 M GuHCl, 35 °C). The range of distributions consistent with the data was generated using the lower and upper confidence limits of $\bar{r}$ and hw.

Representative distance-distribution profiles of the helical and random coil states of S-peptide segments are given in Figure 6. These profiles are normalized by the area and were generated using the values of the lower and higher confidence limits of $\bar{r}$ and hw. Each representation is therefore an envelope of four curves. The distribution is narrow in the helical form (S-protein complex) and wide in random coil form (6 M GuHCl, 35 °C). The broadening of the distribution with the loss of secondary structure is more obvious for Lys(dns)1–Trp 8 than Trp 8–Dap(dns)18 segment.

Anisotropy Decays

The results of tryptophan anisotropy decays of S-peptide under experimental conditions similar to those used in distance-distribution measurements are given in Table VI, and some representative data are shown in Figure 7. We could fit all anisotropy data to two correlation times, one reflecting local tryptophan motions while the larger correlation time described overall motions of the peptide. At 2 °C the S-peptide behaved as a reasonably rigid structure whether it was 50–60% helical (50% TFE), somewhat helical (pH 4.8) or with little secondary structure (pH 8.0 and 6 M GuHCl). About $^2/_3$ of the zero-time or limiting anisotropy was associated with the global motions of the peptide under these conditions. A small but noticeable increase in the amplitude of the local motions was however seen when pH was raised from 4.8 to 8.0. Upon increasing the temperature to 35 °C, the peptide became flexible as we now observed an anisotropy decay which was

Table VI: Anisotropy Decays of Trp 8, S-Peptide[a]

experimental conditions	T (°C)	θ_i (ns)	r_i	r_0[b]
pH 8.0, 50% TFE	2	0.33	0.056	0.262
		4.86	0.206	
pH 4.8	2	0.16	0.073	0.265
		1.98	0.192	
pH 8.0	2	0.23	0.094	0.266
		2.40	0.172	
pH 8.0	35	0.15	0.180	0.265
		1.63	0.085	
pH 8.0, 6 M GuHCl	2	0.29	0.087	0.281
		3.34	0.194	

[a] The excitation wavelength was 297 nm, and the emission was measured through Schott WG 320 and 340-nm interference filters. [b] $r_0 = \sum r_i$ was a variable parameter.

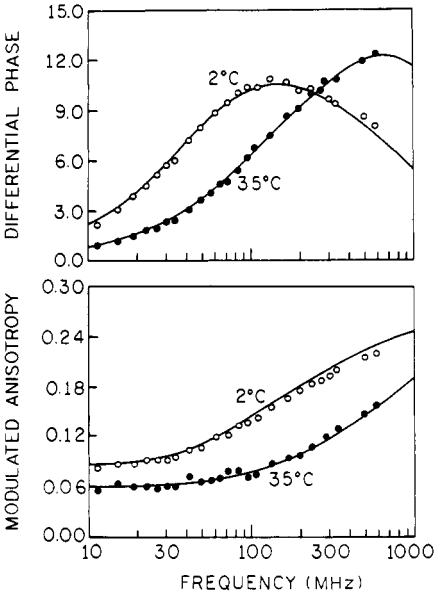

FIGURE 7: Frequency domain anisotropy decays of S-peptide at pH 8.0, 2 °C (○) and 35 °C (●).

primarily associated with the local motions. In general, the trend in the flexibility in S-peptide seen in anisotropy decays is similar to that in distance-distribution parameters. The anisotropy decay of the S-peptide in the presence of 6 M GuHCl at 2 °C is somewhat surprising. Even though the S-peptide is an extended structure in the presence of 6 M GuHCl, rather than behaving like a flexible molecule it behaves more like a rigid structure. This rigidity is reflected in the restricted motions of Trp 8. A similar behavior was also seen in the distance-distribution in the presence of 6 M GuHCl at 2 °C.

DISCUSSION

To make a meaningful assessment of the observed distance distributions in the present study, it is necessary to know the behavior expected for helical and random coil forms of short peptides. In case of polypeptides (residues 50 and longer) and proteins, the statistical mechanical theories of polymer behavior reasonably describe the experimentally observed macroscopic behavior (Tanford, 1968). The Gaussian distribution function is a result of the application of the theory of random walks to the description of a freely joined chain. In case of short oligomer chains (less than 10 bonds), the distribution function is more like a skewed-Gaussian (Flory, 1969). However, there have been only a few fluorescence-based experimental observations where it was possible to discriminate between the Gaussian form and other distributions. Wiczk et al. (1992) using different acceptors, a total of 13 Förster distances, were able to show that a 12 segment long methylene chain was better described by a skewed-Gaussian distribution. Similarly, Rice et al. (1991) reported a Lorentzian rather than a Gaussian distance distribution in case of a rather rigid oligosaccharide. It should be noted that either by experimental design (Wiczk et al., 1992) or due to intrinsic property (Rice et al., 1991) there was no end-to-end diffusion present in these studies. Using same methylene chain and three donor–acceptor pairs, the distance distribution was also examined in a fluid environment. We found that, in the presence of significant end-to-end diffusion, it was not possible to discriminate between a skewed-Gaussian and a Gaussian distribution (Maliwal et al., 1993). In preliminary simulations where intensity decays were generated for a skewed-Gaussian distribution in the presence of end-to-end diffusion, we were not able to discriminate between the Gaussian and the skewed-Gaussian distributions (unpublished observations). Even after two global linkages, both simultaneously present, multiple Förster distances (Maliwal et al., 1993) and an external quencher (Lakowicz et al., 1991), the differences between two distributions were rather modest and the recovered parameters for the skewed-Gaussian had considerable uncertainties. Fortunately, the relative trend remains the same in two analyses. A narrow distribution simulated by skewed-Gaussian will always give a relatively narrower Gaussian distribution. This suggests that the trends we observed, as discussed later, will still be valid and meaningful.

The precise form of the distance distribution functions is less obvious for short peptides, as intrachain interactions, if present, will also significantly influence the distance distributions. Also, there is a paucity of experimental observations. However, we can at least define the limits for $\bar{r}$, hw, and D in case of small peptides from these few published reports. Of the three parameters, the hw is perhaps most sensitive to conformational dynamics. A half-width of 3–4 Å has been reported in the case of a rigid hexapeptide Dns(Pro)$_6$Trp (Lakowicz et al., 1992, 1993) and structured zinc finger peptide (Eis & Lakowicz, 1993). This lower limit for hw in case of a completely helical peptide primarily reflects the flexibility involving the probe linkers and the inherent resolution of the measurements. A hw of about 15 Å was observed in the case of a seven-residue random coil peptide, Dns(Gly)$_6$Trp (Lakowicz et al., 1993). From these values of the hw, we can expect a hw value in the range of 16–18 Å for Lys(dns) 1–Trp 8 segment and about 21–24 Å in the case of Trp 8–Dap(dns)18 segment when they are random coil. The mean distance, $\bar{r}$, for a helical linear peptide can be calculated from 1.4- to 1.5-Å rise per residue (seen in crystal structures). However, for small peptides, it is difficult to generalize the expected $\bar{r}$ for a random coil which to some extent will depend on the particular amino acid sequence of the peptide involved. In case of larger peptides (≥20 residues) the $\bar{r}$ value decreases when a helical peptide becomes random coil (Cheung et al., 1991a; Lakowicz et al., 1992). At room temperature values of $D \leq 10^{-7}$ cm^2/s have been observed in case of peptides longer than 20 residues and with significant secondary structure. An increase of 5–10-fold in D has also been observed upon denaturation by GuHCl and with an increase in temperature (Beals et al., 1991; Lakowicz et al., 1992; Eis & Lakowicz, 1993). It should be noted that the value of D will

also depend on whether it is an isolated short peptide or whether the probes are located in the middle of the protein sequence.

In case of the mean distance for segment 1–8, we did not observe any significant differences in value of $\bar{r}$ when S-peptide changed from highly helical (50% TFE, 2 °C) to essentially random coil with little helical content (pH 8.0, 35 °C). However, some lengthening of the peptide upon loss of helix was observed in the case of the 8–18 segment. In both segments significantly more pronounced lengthening with the loss of helix was seen in the presence of 6 M GuHCl. The behavior of $\bar{r}$ for the S-peptide is different from that of melittin and troponin I where denaturation results in smaller end-to-end distances. For example, the mean distance upon denaturation decreased from 27 to 18 Å in case of melittin segment 1–19 and from 25 to 19 Å in the case of segment 133–158 of troponin I (Lakowicz et al., 1992). However, there are also reports of unchanged $\bar{r}$ upon denaturation in case of C-terminal peptide from RNase (Beals et al., 1991) and 15-residue helical segment of zinc finger peptide (Eis & Lakowicz, 1993). The presence of α-helical structure may either hold the donor and acceptor farther apart, as in the case of melittin, or draw them closer together in other proteins or peptides. These results suggest that the relationship between secondary structure and $\bar{r}$ in case of small peptides is significantly governed by the given amino acid composition and sequence, and a generalized behavior may not be expected.

The structured forms of both segments were rather rigid as seen by the values of $D \leq 1 \times 10^{-7}$ cm^2/s and became more flexible with the loss of helix as seen by the several-fold increase in the D value. As expected, the most flexible form of S-peptide was observed at 35 °C in the presence of 6 M GuHCl. Similar values of D of about 1×10^{-6} cm^2/s at 20 °C in the presence of GuHCl have also been reported for an isolated C-terminal peptide from RNase (Beals et al., 1991), for zinc finger peptide (Eis & Lakowicz, 1993), and for random coil Dns(Gly)$_6$ Trp (Lakowicz et al., 1993). The increase in D with the loss of secondary structure and the increase in temperature from 2 to 35 °C suggest that end-to-end diffusion coefficients in isolated peptides and proteins are sensitive to the conformation and also to their intrinsic stiffness.

The general trend in the hw was similar to that seen in D under comparable experimental conditions. In case of segment 1–8, the hw of 8.6 Å in S-protein complex suggests the presence of considerable conformational heterogeneity. Recall that a hw $\leq$ 4 Å is observed in both rigid and structured peptides (Eis & Lakowicz, 1993; Lakowicz et al., 1992). The most likely contributor to this heterogeneity is Lys(dns) 1 which is not part of the helix (Filippi et al., 1978; Rico et al., 1986; Nelson & Kallenbach, 1989). A similar increase in the hw due to fraying of the terminal residues was also seen in melittin (Lakowicz et al., 1992) and in the case of an α-helical segment of the zinc finger peptide (Eis & Lakowicz, 1993). Also of interest is a broader distribution in the presence of 50% TFE when compared to S-protein complex even though their helical contents are similar. This would point to the restrictions imposed on the conformational disorder by the tertiary structure of a protein. In solution, besides the fraying Lys(dns)1, the salt bridge involving Glu2$^-$–Arg10$^+$ should also add to the conformational heterogeneity. Partial loss of helix is seen in a further increase of the hw to about 14 Å (pH 4.8, 2 °C), and the complete loss of helix is seen by a hw of about 18 Å (pH 8.0, 2 and 35 °C and 6 M GuHCl at 35 °C). The differences in hw and D between pH 4.8 and 8.0 in case of segment 1–8 are good examples of the sensitivity of the distance distributions to the presence of helical structure.

The trend in hw values in segment 8–18 reflects both similarity and differences when compared to 1–8 segment. Unlike segment 1–8, here the hw in the case of S-protein complex is narrower and close to that expected for a structured form. However, similar to that in 1–8 segment, there is an increase in hw as we go from S-protein complex to 50% TFE and to pH 4.8. Another difference between the two segments is the lack of further increase in the hw in segment 8–18 at pH 8.0, 2 and 35 °C. Furthermore, the hw of about 14 Å in the presence of 6 M GuHCl at 35 °C is significantly smaller than that expected for a 11-residue random coil peptide. The hw results for segment 8–18 are another indication that in small peptides the specific amino acid composition will have a significant bearing on the relationship between distance distributions and the conformational disorder.

We observed a rather surprising behavior for both segments at 2 °C in the presence of 6 M GuHCl. The values of D and hw were among the smallest in the series and were comparable to that in S-protein complex. These observations along with an increased $\bar{r}$ indicate that, at 2 °C in the presence of 6 M GuHCl, S-peptide is an extended and rigid structure of limited conformational heterogeneity. The results from the anisotropy decays which are discussed later also support this. Usually one expects peptides in the presence of 6 M GuHCl to become random coil. We do not have any obvious explanation for this contrary behavior. These results do, however, suggest that at least part of the conformational heterogeneity in the presence of 50% TFE and pH 4.8 at 2 °C is likely to be due to extrachain interactions such as Glu2$^-$–Arg10$^+$ and Trp8–His12$^+$. These interactions will be abolished in the presence of 6 M GuHCl.

The anisotropy decays in general showed the same trend as that seen in distance distributions. As Trp 8 is almost in the middle of the peptide as well as the helix, it should be sensitive to both the loss of helical structure as well as to the intrinsic flexibility of S-peptide. At 2 °C, in both helical and extended structures, the anisotropy decays were dominated by overall peptide rotational motions. In contrast, at 35 °C the local motions of the Trp 8 residue accounted for most of the anisotropy decays. Overall, the anisotropy decays indicate S-peptide to be of limited flexibility at 2 °C and to become highly flexible upon raising the temperature to 35 °C. The behavior of S-peptide is very similar to that of Trp 19 in melittin (25 residues) when in comparable conformational states (Lakowicz et al., 1990).

We were also interested in determining the relative stabilities of helix toward the N- and C-terminals. There is some indications that at pH 4.8 most of the remaining helix is located in segment 1–8. This is reflected in further broadening of hw in this segment upon raising the pH to 8.0. However, an unequivocal conclusion is not possible due to several reasons. First is the positions of the acceptor, which, in hindsight, should have been on residues 2 and 14 or 15, rather than on 1 and 18. The fraying of N-terminal residue significantly broadened hw in the case of segment 1–8 even in the helical state. Similarly, the result for segment 8–18 reflects both the process of loss of helix involving residues 8–13 and the behavior of remaining residues which are outside the helix. The trend, however, does suggest that the segment 8–18 is more rigid than the segment 1–8. We are also somewhat cautious in our interpretation of the results due to the presence of significant uncertainties in the recovered parameters. Even though an external quencher acrylamide was used to enhance the resolution (Lakowicz et al., 1991), we were restricted to 2–3-fold quenching of donor fluorescence due to its modest quantum yields. A better quantum yield fluorophore would have allowed

us to more quenching and consequently better resolution. However, these problems are not intrinsic to FRET distance distribution method. An enhanced resolution can also be obtained by using sensitized acceptor fluorescence (Beechem & Haas, 1989) or by varying R_0 using more than one acceptor (Maliwal et al., 1993). Some combinations of these approaches can also be used. Similarly, in place of tryptophan as donor, it should be possible to use an appropriate amino acid analog with an extrinsic probe. By selecting a suitable probe and locating it at suitable positions in a peptide sequence, significant insight into both the conformational dynamics and behavior of a localized helix should be available from FRET distance distributions.

ACKNOWLEDGMENT

We express our appreciation to Drs. M. L. Johnson and J. Kuśba for providing the software needed for the distance distribution analysis.

REFERENCES

Amir, D., & Haas, E. (1988) *Biochemistry 27*, 8889–8893.
Anfinsen, C. B. (1973) *Science 181*, 223–230.
Barrick, D., & Baldwin, R. L. (1993) *Protein Sci. 2*, 869–876.
Beals, J. M., Haas, E., Krausz, S., & Scheraga, H. A. (1991) *Biochemistry 30*, 7680-7692.
Bierzynski, A., Kim, P. S., & Baldwin, R. L. (1982) *Proc. Natl. Acad. Sci. U.S.A. 79*, 2470–2474.
Brown, J. E., & Klee, W. A. (1971) *Biochemistry 10*, 470–476.
Cheung, H. C., Gryczynski, I., Malak, H., Wiczk, W., Johnson, M. L., & Lakowicz, J. R. (1991a) *Biophys. Chem. 40*, 1–17.
Cheung, H. C., Wang, C.-K., Gryczynski, I., Wiczk, W., Laczko, G., Johnson, M. L. & Lakowicz, J. R. (1991b) *Biochemistry 30*, 5238–5247.
Connelly, P. R., Varadarajan, R., Sturtevant, J. M., & Richards, F. M. (1990) *Biochemistry 29*, 6108–6114.
Eis, P. S., & Lakowicz, J. R. (1993) *Biochemistry 32*, 7981–7993.
Filippi, B., Boring, G., & Marchiori, F. (1976) *J. Mol. Biol. 106*, 315–324.
Filippi, B., Boring, G., Moretto, V., & Marchiori, F. (1978) *Biopolymers 17*, 2545-2559.
Flory, P. J. (1969) *Statistical Mechanics of Chain Molecules*, Interscience, New York.
Gans, P. J., Lyu, P. C., Manning, M. C., Woody, R. W., & Kallenbach, N. R. (1991) *Biopolymers 31*, 1605–1614.
Gierasch, L. M., & King, J., Eds. (1989) *Protein Folding*, AAAS, Washington, D.C.
Grinvald, A., Haas, E., & Steinberg, I. Z. (1972) *Proc. Natl. Acad. Sci. U.S.A. 69*, 2273–2277.
Gryczynski, I., Wiczk, W., Johnson, M. L., Cheung, H. C., Wang, C.-K., & Lakowicz, J.R. (1988) Biophys. J. 54, 577–586.
Haas, E., Wilchek, M., Katchalski-Katzir, E. & Steinberg, I. Z. (1975) *Proc. Natl. Acad. Sci., U.S.A. 72*, 1807–1811.
Haas, E., Katchalski-Katzir, E., & Steinberg, I. Z. (1978) *Biopolymers 17*, 11–31.
Haas, E., McWherter, C. A., & Scheraga, H. A. (1988) *Biopolymers 27*, 1–21.
Jaenicke, R. (1991) *Biochemistry 30*, 3147–3161.
Kim, P. S., & Baldwin, R. L. (1982) *Annu. Rev. Biochem. 51*, 459–489.
Kuśba, J. and Lakowicz, J. R. (1993) *Methods Enzymol.* (in press).
Laczko, G., Gryczynski, I., Gryczynski, Z., Wiczk, W., Malak, H. & Lakowicz, J. R. (1990) *Rev. Sci. Instrum. 61*, 2331–2337.
Lakowicz, J. R., Laczko, G., Cherek, H., Gratton, E., & Limkeman, M. (1984) *Biophys. J. 46*, 463–477.
Lakowicz, J. R., Gryczynski, I., Cheung, H. C., Wang, C.-K., Johnson, M. L., & Joshi, N. (1988) *Biochemistry 27*, 9145–9160.
Lakowicz, J. R., Gryczynski, I., Wiczk, W., Laczko, G., Prendergast, F. C., & Johnson, M. L. (1990) *Biophys. Chem. 36*, 99–115.
Lakowicz, J. R., Kusba, J., Gryczynski, I., Wiczk, W., Szmacinski, H., & Johnson, M.L. (1991) *J. Phys. Chem. 95*, 9654–9660.
Lakowicz, J. R., Kusba, J., Gryczynski, I., Szmacinski, H., & Johnson, M. L. (1992) *Tech. Protein Chem. 3*, 429–436.
Lakowicz, J. R., Gryczyński, I., Kuśba, J., Wiczk, W., Szmacinski, H., & Johnson, M. L. (1993) *Photochem. Photobiol.* (in press).
Levinthal, C. (1968) *J. Chim. Phys. Phys.-Chim. Biol. 65*, 44–45.
Maliwal, B. P., & Lakowicz, J. R. (1986) *Biochim. Biophys. Acta. 873*, 161–172.
Maliwal, B. P., Kuśba, J., Wiczk, W., Johnson, M. L., & Lakowicz, J. R. (1993) *Biophys. Chem. 46*, 273–281.
Merutka, G., Shalongo, W., & Stellwagen, E. (1991) *Biochemistry 30*, 4245–4248.
Montelione, G. T., & Scheraga, H. A. (1989) *Acc. Chem. Res.* 22, 70–76.
Nelson, J. W., & Kallenbach, N. R. (1986) *Proteins 1*, 211–217.
Nelson, J. W., & Kallenbach, N. R. (1989) *Biochemistry 28*, 5256–5261.
Osterhout, J. J., Baldwin, R. L., York, E. J., Stewart, J. M., Dyson, J. H., & Wright, P. E. (1989) *Biochemistry 28*, 7059–7064.
Qian, H., & Schellman, J. A. (1992) *J. Phys. Chem. 96*, 3987–3994.
Rice, K. G., Wu, P., Brand, L., & Lee, Y. C. (1991) *Biochemistry 30*, 6646–6655.
Rico, M., Santoro, V., Bermejo, F. J., Herranz, J., Nieto, J. C., Gallego, E. & Jimenez, M. A. (1986) *Biopolymers 25*, 1031–1053.
Scholtz, J. M. Qian, H., York, E. J., Stewart, J. M., & Baldwin, R. L. (1991) *Biopolymers 31*, 1463–1470.
Shoemaker, K. R., Kim, P. S. Brems, D. N., Marqusee, S., York, E. J., Chaiker, I. M., Stewart, J. M., & Baldwin, R. L. (1985) *Proc. Natl. Acad. Sci. U.S.A. 82*, 2349–2353.
Shoemaker, K. R., Kim, P. S., York, E. J., Stewart, J. M., & Baldwin, R. L. (1987) *Nature 326*, 563–567.
Shoemaker, K. R., Fairman, R., Schultz, D. A., Robertson, A. D., York, E. J., Stewart, J. M., & Baldwin, R. L. (1990) *Biopolymers 29*, 1–11.
Steiner, R. F. (1991) in *Topics in Fluorescence Spectroscopy: Principles* (Lakowicz, J. R., Ed.) Vol. 2, pp 1–51, Plenum Press, New York.
Strehlow, K. G., & Baldwin, R. L. (1989) *Biochemistry 28*, 2130–2133.
Sueiki, M., Lee, S., Powers, S. P., Denton, J. B., Konishi, Y., & Scheraga, H. A. (1984) *Macromolecules 17*, 148–155.
Tanford, C. (1968) *Adv. Protein Chem. 23*, 121–282.
Wetlaufer, D. B. (1981) *Adv. Protein Chem.* 34, 61–92.
Wiczk, W., Eis, P. E., Fishman, M. N., Johnson, M. L., & Lakowicz, J. R. (1991) *J. Fluoresc. 1*, 273–286.
Wright, P. E., Dyson, H. J., & Lerner, R. A. (1988) *Biochemistry 27*, 7167–7175.
Zimm, B. H., & Bragg, K. J. (1959) *J. Chem. Phys. 31*, 526–535.